Energy Pathways in Plasma-Assisted Ignition of Ammonia

Raphael J. Dijoud* and Carmen Guerra-Garcia †
Massachusetts Institute of Technology, Cambridge, MA, 02139

This work presents a numerical model to evaluate the energy deposition pathways activated during plasma-assisted ignition of a stoichiometric ammonia/air mixture at atmospheric conditions. To that end, zero-dimensional simulations are conducted of ignition by nanosecond repetitively pulsed discharges (NRPD), for which a detailed energy tracking is performed from the electrical input to the mechanisms that directly influence ignition. The analysis of the plasma energy deposition pathways is relevant to gain insight into complex plasma kinetic mechanisms and help optimize actuation strategies. Results show that the main pathways activated are: (i) slow-gas heating, (ii) fast-gas heating, (iii) dissociation of NH_3 into NH_2, (iv) dissociation of O_2, and (v) dissociation of NH_3 into NH. The exact proportion of energy deposited in each pathway is highly dependent on the reduced electric field profile, in particular the "down-slope" dominates the energy breakdown. The influence of the reduced electric field magnitude is studied for square pulses. The correlation between the various plasma energy deposition pathways and NO_x emissions is quantified.

I. Introduction

The extensive use of hydrocarbon fuels in power generation and transportation is a main contributor to global warming, as such fuels release carbon dioxide into the atmosphere which exacerbates the planet's greenhouse effect. Efforts have been conducted to find alternative, "greener", fuels that satisfy industrial requirements, especially those with a high energy density. Although some challenges remain to minimize the greenhouse gases emitted during its production, ammonia (NH_3) is a promising fuel alternative for some applications as it has a high energy density, it does not directly release carbon dioxide when burnt, and the worldwide production and distribution of ammonia already exist. However, ammonia combustion brings new challenges compared to hydrocarbon fuels, especially it has: (i) a lower specific energy, (ii) a lower laminar burning speed, (iii) a higher auto-ignition temperature, and (iv) a larger Minimum Ignition Energy (MIE). Because of these limitations, ammonia has often been studied as a fuel when mixed with other more reactive fuels such as hydrogen or methane. In addition, ammonia produces large amounts of nitrogen oxides, NO_x, which will need to be abated or mitigated before this fuel can be considered as an option. Plasma assistance can help address the combustion and environmental challenges of ammonia.

Plasma-Assisted Ignition (PAI) is the use of non-equilibrium plasma to modify and improve ignition processes. Plasma discharges are often generated by applying high voltage pulses, reaching hundreds of Townsend locally, of nanosecond duration and repeated at kilohertz frequencies, the so-called Nanosecond Repetitively Pulsed Discharge (NRPD) technique. This strategy enables new chemical reactions as high-energy electrons accelerated by the electric field collide with molecules, leading to an increase in translational and vibrational temperatures, electronic excitation, ionization, and dissociation. Eventually, these various effects relax on different timescales and lead to an increase in overall gas temperature and seeding of radicals. Ignition and flame propagation with plasma assistance have been extensively studied both experimentally and numerically. Regarding ignition, plasma assistance has been found to lower the Ignition Delay Time (IDT) [1, 2], reduce the Minimum Ignition Energy (MIE) [3, 4], improve ignition in lean conditions [5, 6], and allow ignition to occur in high-speed flows [7, 8], among other benefits [9–11]. Research on plasma-assisted combustion has mostly focused on air-small hydrocarbon fuel (methane, ethylene), or air-hydrogen, combustion.

Research on plasma-assisted combustion for ammonia is recent but is capturing the attention of the community and the literature in this sub-field is growing fast. In 2018, a research group in Japan developed a kinetic mechanism for ammonia and conducted simulations on the effect of plasma assistance on the laminar burning velocity of ammonia flames [12]. They found that the flame speed could be increased up to 20%. In 2021, several papers were released by different research groups presenting numerical and experimental results related to ammonia combustion [13–15].

*Ph.D. Candidate, Department of Aeronautics and Astronautics, rdijoud@mit.edu, AIAA Student Member.
†Associate Professor, Department of Aeronautics and Astronautics, guerrac@mit.edu, AIAA Senior Member.

Results include extension of lean blowout limits [13, 15], reduction of ignition delay time of about 50% [13, 14], and, more interestingly, a reduction of NO_x emissions of the flame [15] by the plasma. This result is extremely promising because, for hydrocarbon combustion, plasma has typically increased the NO_x produced through new reaction pathways activated by the plasma, which is undesirable. In 2022, Shahsavari et al. [16] conducted a parametric study to map the performance of plasma assistance on ammonia combustion. Other works have been conducted in 2023 [17] and 2024 [18, 19] looking at PAI performance and NO_x emissions, as well as suppression of combustion dynamics and reduction of emissions in ammonia/methane flames [20].

Research on applications of plasma-assistance in ammonia flames is at its early stages, many phenomena are yet to be explained, and the technology is yet to be developed and demonstrated. First, although significant progress has been made recently [15, 17, 19], the mechanisms of NO_x formation and consumption triggered by the plasma need further study, especially through a detailed analysis of the chemical pathways enabled by the plasma. Second, the energy deposition pathways actuated by the plasma are yet to be characterized and quantified depending on the conditions, which can help optimize and design actuation strategies that enhance combustion performance while keeping emissions at a minimum. Our ongoing computational efforts on this problem are presented in this paper.

II. Methods: Zero-Dimensional Plasma-Ignition Simulation

A. Model Architecture

The zero-dimensional plasma chemical kinetic solver developed in our lab has been presented and used in previous works [21–26]. It contains two distinct reactor models solving at different timescales, and combined using an operator splitting scheme. The first reactor sub-model solves the plasma kinetics on the sub-ns timescale, using the Boltzmann solver BOLSIG [27] embedded into the constant-volume chemical kinetics solver ZDPlasKin [28]. The second reactor sub-model uses the Cantera framework [29] to solve for the sub-μs timescale chemical kinetics that occur between ground-state molecules undergoing combustion chemistry. The thermodynamic properties of the various chemical species are estimated using the NASA polynomials [30]. Within ZDPlasKin, the energy equation is also enabled to account for energy deposition during the pulse. The BOLSIG solver [27] uses the Local Field Approximation (LFA) with a two-term approximation of the electron energy distribution function, which constitutes an acceptable approximation for atmospheric pressure plasmas.

B. Chemical Kinetics

In this work focusing on plasma-assisted combustion of ammonia, we adopted the plasma and combustion kinetics introduced by Zhong et al. in 2023 [31]. In this paper, the authors proposed a comprehensive plasma kinetic mechanism for plasma-assisted oxidation of ammonia with a total of 894 reactions and 74 chemical species tracked. This mechanism was fine-tuned using experimental data of low-pressure oxidation of ammonia at ambient temperature. The authors validated the numerical predictions of densities of N_2O, NO, and OH for three different gas compositions. The same mechanism was later used by Mao et al. [19] to study numerically the performance of plasma-assisted ignition in ammonia/air mixtures at atmospheric pressure. For consistency, the combustion model used in this paper is the accompanying combustion model developed by the Princeton group [31].

C. Energy Tracking

The applied voltage waveform, which is an input of the model in the form of a reduced electric field profile, communicates energy to the gas by accelerating free electrons that undergo collisions with heavy particles. Those collisions can be either elastic or inelastic. Thermal energy released by elastic collisions is often much smaller than energy communicated through inelastic collisions in our discharge and gas conditions. Inelastic collisions are collisions where part of the energy of the incoming electron is consumed into (i) excitation (rotational, vibrational, or electronic), (ii) ionization, or (iii) direct dissociation of the molecules. Most prior studies focus on the energy deposition pathways activated during the electron-heavy collision stage, which can typically be retrieved directly from the Boltzmann solver without needing to solve the kinetics. An example of the energy deposition pathways breakdown at the electron-heavy collision step is shown in figure 1 for an ammonia-air mixture.

The study of the pathways activated during the energy transfer between electrons and heavy particles, as shown in figure 1, allows us to get insight into what species are produced during the collisions, essentially identifying the plasma-activated species. However, it is also limiting in its ability to help us understand the effect of the plasma on the

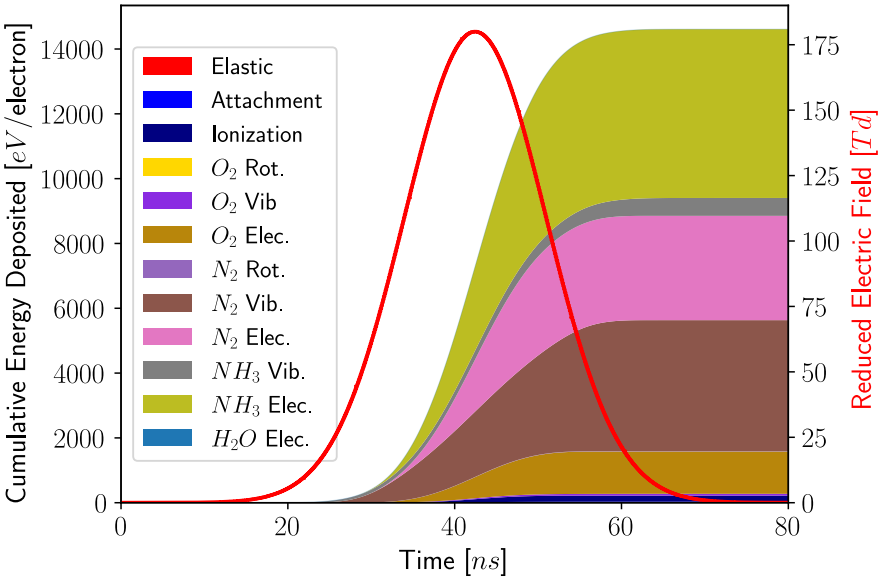

Fig. 1 Example of a balance of the energy deposited per electron integrated over the pulse time for stoichiometric ammonia-air at 300 K **and** 1 atm**. Electron collisions cross-sections from [31].**

gas: (i) the pathways activated will continue to evolve in simulations as gas conditions change, (ii) this method only gives us relative values, and we do not know how much energy is going into each pathway, and (iii) more importantly, the final effects on the gas, which are the most relevant to quantify combustion enhancement, remain unknown (for instance, electronic excitation could lead to fast-gas heating or dissociative quenching). To resolve those issues and complete the analysis, we should track the energy deposited as it evolves during subsequent chemical reactions between heavy-heavy particles.

The energy transfers within the plasma chemical kinetic mechanism can be categorized into three types: (i) the energy spent to form unstable species such as excited species or ions, (ii) the energy spent in dissociating stable molecules into smaller molecules and atoms, and (iii) the energy spent into raising the temperature of the gas. Regarding category (i), the energy stored at each instant in an excited species or ion k_p relative to their ground state, noted $\mathcal{E}_{k_p}$, can be computed using the number density n_{k_p} and the excess energy ϵ_{k_p} as:

$$\mathcal{E}_{k_p}(t) = n_{k_p}(t)\epsilon_{k_p} \tag{1}$$

For instance, the first electronic level of molecular nitrogen, $N_2(A)$, has an energy of $\epsilon_{k_p} = 6.17\ eV$ with respect to the ground state, $N_2(X)$. For the other two categories, namely dissociation and gas heating, the evolution of the energy spent in each process α, written $\mathcal{E}_\alpha$, must be manually specified within the plasma mechanism for each reaction. Processes include rotational-translational relaxation (heating), vibrational-translational relaxation (*slow* gas heating), electronic quenching (*fast* gas heating), but also dissociation pathways, such as $O_2 \rightarrow O + O$ or $NH_3 \rightarrow NH + H_2$. If $\delta\epsilon^{\alpha}_{r_p}$ refers to the change in energy stored in process α for reaction r_p, than we can write:

$$\frac{d\mathcal{E}_\alpha}{dt}(t) = \sum_{r_p} R_{r_p}(t)\delta\epsilon^{\alpha}_{r_p} \tag{2}$$

Where R_{r_p} is the rate of reaction r_p. A more detailed explanation of the methodology, along with examples for methane-air mixtures, has been recently published by our group [26].

Following this methodology for tracking energy deposition pathways beyond the electron-heavy interactions, the list of energy pathways directly depends on the plasma chemical kinetic mechanism used. Using the kinetics from Zhong et al. [31], we classified the interactions into $\sim$ 130 distinct pathways. A list of the most important pathways is given in table 1.

Thermal Pathways	Kinetic Pathways	Others
R-T Relaxation	$NH_3 \rightarrow NH_2 + H$	Radiation Out
V-T Relaxation	$NH_3 \rightarrow NH + H_2$	
Electronic Quenching	$O_2 \rightarrow O + O$	
Ion-e Attachment	$N_2 \rightarrow N + N$	
Neutral-e Attachment	$N + NH_3 \rightarrow NH_2 + NH$	
Anion Neutralization	$OH + H \rightarrow H_2O$	

Table 1 Main energy deposition pathways activated in ammonia/air combustion, using the kinetic mechanism from [31].

III. Results: Plasma Energy Deposition Pathways in Ammonia Combustion

A. Example Case in Stoichiometric Ammonia/ Air

We used the zero-dimensional numerical tool described in section II to model the effect of 20 high-voltage nanosecond pulses applied at 20 kHz in a stoichiometric ammonia/air mixture at atmospheric conditions. Each pulse voltage profile follows a Gaussian shape as follows:

$$\frac{E}{N}(t) = (E/N)_{max}\, e^{-\frac{1}{2}\left(\frac{t-3\sigma}{\sigma}\right)^2} \tag{3}$$

Where $\sigma = \frac{FWHM}{\sqrt{2\ln 2}}$, $FWHM = 15\ ns$, and $(E/N)_{max} = 190\ Td$. The initial electron density is $10^3\ cm^{-3}$. If and when the energy deposited during a single pulse reaches 200 $mJ \cdot cm^{-3}$, the reduced electric field is linearly relaxed to zero on the timescale of the inverse plasma frequency to emulate electric field shielding. We used the plasma and combustion mechanisms by Zhong et al. [31] (see section II.B).

Figure 2a shows the time-dependent evolution of the main chemical species and gas temperature, and figure 2b shows the time-dependent reduced electric field and breakdown of the energy deposition pathways for the 17-th pulse of the pulse train. Since the pulses reach a periodic evolution, pulse 17-th is representative of the behavior of all pulses in the pulse-train except the initial ones as the electron population is built.

Figure 2b illustrates that the instantaneous breakdown of the cumulative energy stored in each pathway is highly time-dependent. First of all, it is important to note that most of the energy of the pulse is deposited during the "down-slope" of the pulse waveform, i.e., after the ionization threshold has passed and the electron density has increased significantly. Therefore, it can be assumed that the shape of the pulse profile during the "up-slope" has little effect on the overall amount of energy deposited and the pathways actuated, compared to the down-slope rate. During the pulse, on a timescale up to a few tens of ns, the energy is mainly deposited into electronic (42%) and vibrational (47.4%) states. The energy deposited into electronic states is transferred very fast into dissociation of NH_3 (26.3%) and O_2 (7.3%) molecules through dissociative quenching, and into fast-gas heating (15.7%). At the end of the pulse, almost no electronically excited states remain. The vibrational states relax into heating through V-T relaxation (*slow* gas heating), on a much longer timescale up to a few tens of μs. Because the ionization fraction remains low in this case (peaking at $4 \cdot 10^{-6}$), the amount of energy stored in ions and the amount of heating released by ion-electron attachment is negligible. However, it is important to reiterate that, although the "up-slope" of the pulse profile has little effect on the gas energy-deposition pathways, the "down-slope" dictates which deposition pathways are activated and dominate. Therefore, different pulse shape profiles can lead to different conclusions from an energy tracking analysis standpoint, as activated pathways depend on the reduced electric field time-dependent profile. This information could potentially be used to optimize the energy delivery process.

B. Influence of Reduced Electric Field Magnitude

The energy pathways activated during a discharge depend on various parameters, including gas composition, electron density, pulse repetition frequency, and reduced electric field. Previous works have shown that the value of the reduced electric field, especially during the "downside" profile of the pulse (i.e. the part of the pulse where the electron density is high), directly affects what pathways are activated [26].

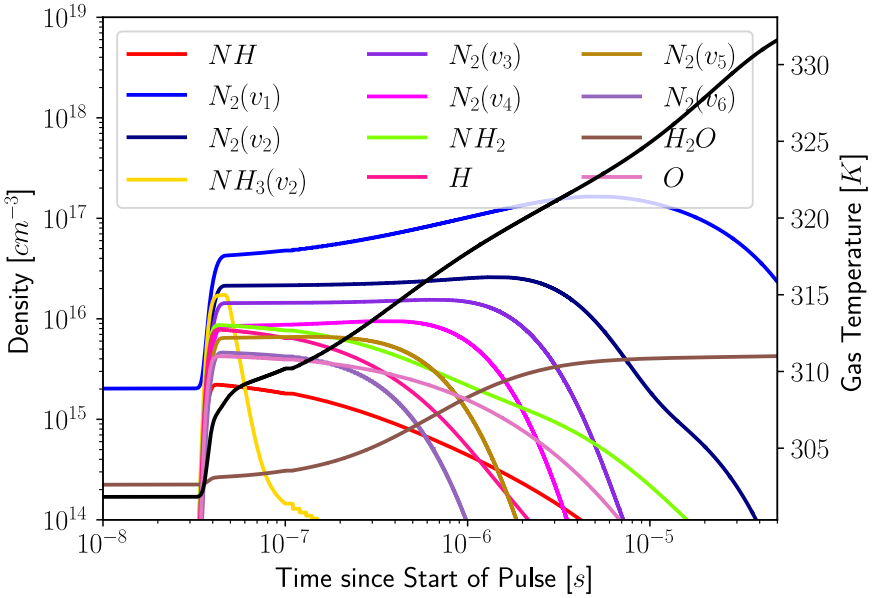

(a) Main Species and Temperature

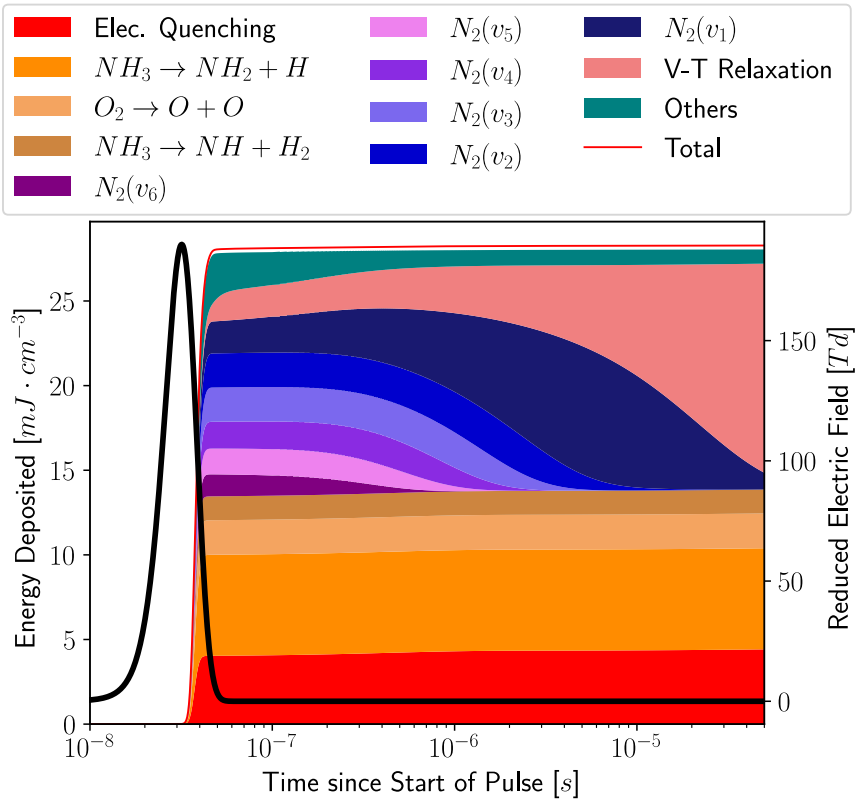

(b) Energy Deposition Pathways and Reduced Electric Field Profile

Fig. 2 Species and energy deposition pathways during the 17-th pulse of a 20 kHz pulse train applied in stoichiometric ammonia/air at atmospheric conditions.

Figure 3 shows the evolution of the contributions of the main energy deposition pathways as a function of the reduced electric field. For each case, 10 square pulses are applied at 20 kHz in a stoichiometric ammonia/air mixture at atmospheric conditions. The width of the pulse is adapted at each iteration so that the energy deposited remains around 10 $mJ \cdot cm^{-3}$ per pulse. The cumulative pathways breakdown is taken after 1 s. Note that for this exercise, the voltage pulse is different from that described in section III. This choice removes the influence of the rate of change in the reduced electric field, by considering a constant reduced electric field magnitude during pulse application. When the energy balance is conducted, the sum of all the cumulative energy deposited in every pathway should match the total electric energy consumed by the discharge. In our simulations, a small discrepancy, on the order of 1% was observed, which could be caused by the accumulation of numerical errors. The corresponding error over the sum of all the contributions can be translated into an error on the energy stored in each individual pathway. This error is shown on figure 3 as error bars.

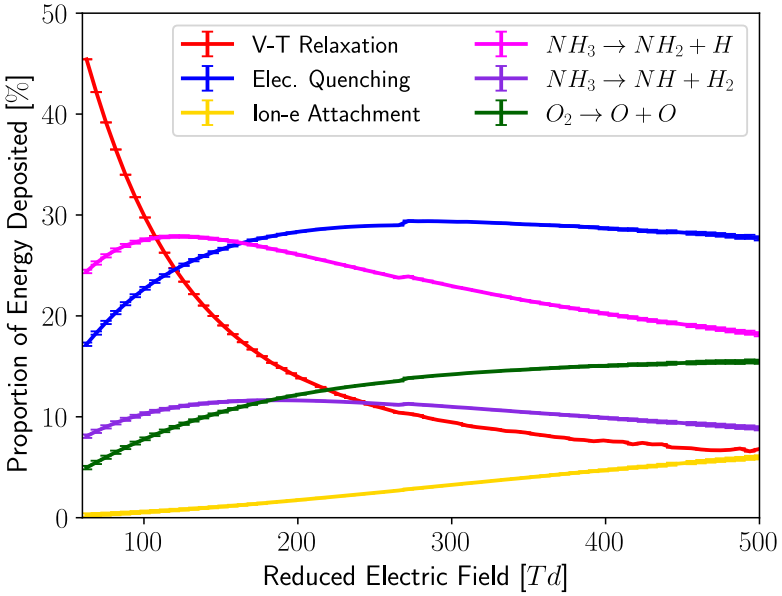

Fig. 3 Main plasma energy deposition pathways activated in stoichiometric NH_3/air at atmospheric conditions as a function of applied reduced electric field.

Figure 3 shows that, at low reduced electric fields, the vibrational-translational relaxation, or *slow* gas heating, is largely dominant, contributing over 45% of the energy deposited around 65 Td. As the reduced electric field increases, pathways related to electronic excitation gain more importance. Those pathways include *fast* gas heating (electronic quenching), but also the dissociation reactions of NH_3 and O_2 which are enabled through dissociative quenching of electronically excited molecules. For very high reduced electric fields, above 250 Td, the contribution of the thermal energy released during ion-electron attachment increases, until reaching around 8% at 500 Td.

C. Correlation with NO_x Emissions

Ensuring that plasma assistance does not increase the NO_x emissions is paramount in allowing the technology to be of value to the industry. Therefore, studying how the plasma energy deposition pathways affect or correlate with the NO_x emissions is directly relevant to the optimization of the plasma actuation strategy. We used the dataset of plasma-assisted ignition cases presented in section III.B to generate a correlation map between each pathway and the NO_x emissions. More specifically, we quantify the correlation between the share of energy that is deposited into a specific plasma pathway with the NO_x concentration, through a Pearson correlation coefficient. NO_x concentration is taken as the sum of the mole fractions of NO and NO_2 after ignition, which is independent of time in adiabatic zero-dimensional simulations. Across our simulation cases, the NO_x concentration after ignition remains in a small range between 6000 and 6200 ppm depending on the applied reduced electric field. The results are shown in figure 4

for the main plasma energy deposition pathways, along with the corresponding p-value (statistical significance).

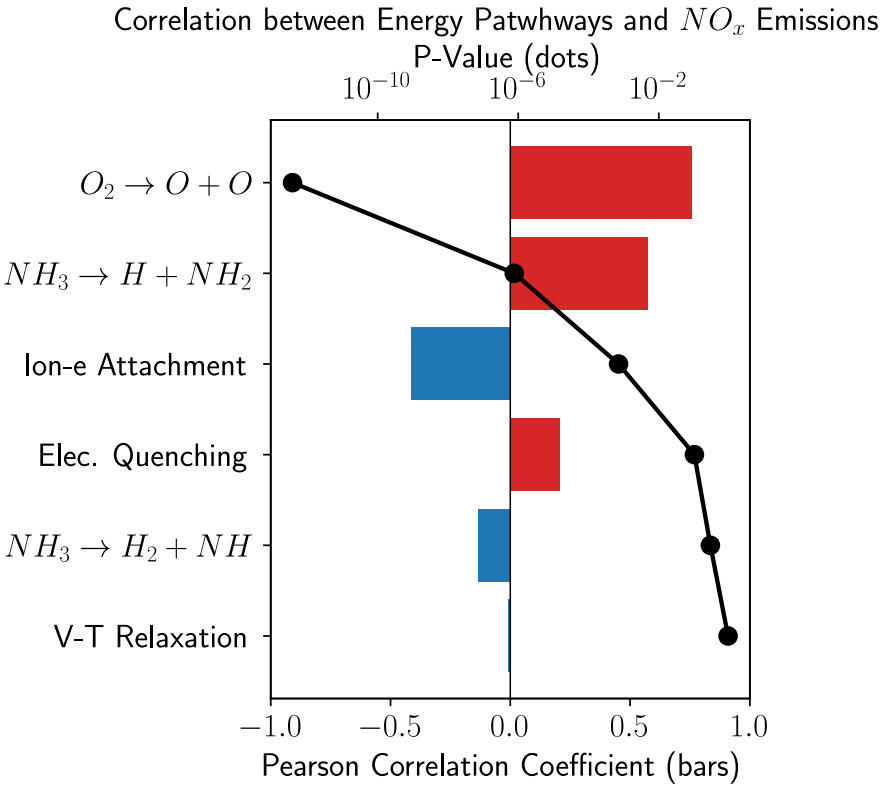

Fig. 4 Pearson correlation coefficients between the main plasma energy pathways and NO_x emissions.

Results shown in figure 4 reveal that energy pathways directly associated with gas heating, such as electronic quenching (fast-gas heating), vibrational-translational relaxation (slow-gas heating), or ion recombination, do not significantly correlate with NO_x emissions. Only two pathways seem to show a high correlation with NO_x production: dissociation of O_2 (positive correlation), and dissociation of NH_3 into NH_2 (positive correlation). The dissociation of O_2 generates O atoms that can react with ground-state or excited N_2 to form NO, therefore opening a new path towards the generation of NO. Whereas the increased production of NO triggered by the dissociation of O_2 comes at no surprise, the dependency of NO_x formation with the dissociation of NH_3 into NH_2 needs more explanation. NH_2 is often thought to contribute to de-NO_x reactions, such as $NH_2 + NO \rightarrow NNH + OH$ and $NH_2 + NO \rightarrow N_2 + H_2O$. However, Zhong et al. [31] showed that, for their combustion mechanism (that we used in this work), NH_2 was also a significant contributor to NO formation through the formation of the intermediate species HNO. In our work, the Pearson correlation coefficient for this pathway remains low (below 0.6), but is still significant. The observed discrepancy between our results and those from the community could be explained in various ways: (i) the range of NO_x emissions across the dataset is too small, leading to unreliable correlation maps, (ii) the suppression of NO_x by NH_2 is compensated by another unknown effect of the plasma, (iii) the combustion or plasma kinetics have missing or erroneous pathways for NO production and consumption. At the time of writing this paper, further studies are in progress to understand this discrepancy.

IV. Conclusion

In this work, simulations of zero-dimensional plasma-assisted ignition by NRPD of stoichiometric ammonia/air mixtures at atmospheric conditions are conducted to study the plasma energy deposition pathways in ammonia combustion. Results show that the main pathways actuated are: (i) slow-gas heating, (ii) fast-gas heating, (iii) dissociation of NH_3 into NH_2, (iv) dissociation of O_2, and (v) dissociation of NH_3 into NH. The influence of the reduced electric field is quantified, revealing that the energy deposited in each pathway is highly dependent on the applied voltage pulse profile, particularly during the "down-slope" of the voltage pulse. At very high reduced electric

fields, gas heating from recombination of ions becomes significant. The correlations between energy pathways activated and NO_x emissions are also presented. Results suggests that both the dissociation of O_2 and the production of NH_2 correlates positively with the formation of NO_x. Further work on investigating the kinetics and pathways of ammonia is needed to articulate an optimal plasma actuation strategy in terms of ignition/combustion enhancement and emissions reductions.

Acknowledgments

This research was funded by the National Science Foundation (NSF), under Award Number 2339518.

References

[1] Bozhenkov, S. A., Starikovskaia, S. M., and Starikovskii, A. Y., "Nanosecond gas discharge ignition of H2- and CH4- containing mixtures," *Combustion and Flame*, Vol. 133, No. 1-2, 2003, pp. 133–146. https://doi.org/10.1016/S0010-2180(02)00564-3.

[2] Kosarev, I. N., Aleksandrov, N. L., Kindysheva, S. V., Starikovskaia, S. M., and Starikovskii, A. Y., "Kinetics of ignition of saturated hydrocarbons by nonequilibrium plasma: CH4-containing mixtures," *Combustion and Flame*, Vol. 154, No. 3, 2008, pp. 569–586. https://doi.org/10.1016/j.combustflame.2008.03.007.

[3] Tropina, A. A., Uddi, M., and Ju, Y., "On the effect of nonequilibrium plasma on the minimum ignition energy: Part 2," *IEEE Transactions on Plasma Science*, Vol. 39, No. 12, 2011, pp. 3283–3287. https://doi.org/10.1109/TPS.2011.2160570.

[4] Singleton, D., Pendleton, S. J., and Gundersen, M. A., "The role of non-thermal transient plasma for enhanced flame ignition in C2H4-air," *Journal of Physics D: Applied Physics*, Vol. 44, No. 2, 2011. https://doi.org/10.1088/0022-3727/44/2/022001.

[5] Pineda, D. I., Wolk, B., Sennott, T., Chen, J. Y., Dibble, R. W., and Singleton, D., "Nanosecond pulsed discharge ignition in a lean methane-air mixture," *Laser Ignition Conference 2015*, 2015. https://doi.org/10.1364/lic.2015.t5a.2.

[6] Lovascio, S., Hayashi, J., Stepanyan, S., Stancu, G. D., and Laux, C. O., "Cumulative effect of successive nanosecond repetitively pulsed discharges on the ignition of lean mixtures," *Proceedings of the Combustion Institute*, Vol. 37, No. 4, 2019, pp. 5553–5560. https://doi.org/10.1016/j.proci.2018.06.029.

[7] Do, H., Cappelli, M. A., and Mungal, M. G., "Plasma assisted cavity flame ignition in supersonic flows," *Combustion and Flame*, Vol. 157, No. 9, 2010, pp. 1783–1794. https://doi.org/10.1016/j.combustflame.2010.03.009.

[8] Do, H., Im, S. K., Cappelli, M. A., and Mungal, M. G., "Plasma assisted flame ignition of supersonic flows over a flat wall," *Combustion and Flame*, Vol. 157, No. 12, 2010, pp. 2298–2305. https://doi.org/10.1016/j.combustflame.2010.07.006.

[9] Ju, Y., and Sun, W., "Plasma assisted combustion: Dynamics and chemistry," *Progress in Energy and Combustion Science*, Vol. 48, 2015, pp. 21–83. https://doi.org/10.1016/j.pecs.2014.12.002.

[10] Starikovskaia, S. M., "Plasma assisted ignition and combustion," *Journal of Physics D: Applied Physics*, Vol. 39, No. 16, 2006. https://doi.org/10.1088/0022-3727/39/16/R01.

[11] Starikovskiy, A., and Aleksandrov, N., "Plasma-assisted ignition and combustion," *Progress in Energy and Combustion Science*, Vol. 39, No. 1, 2013, pp. 61–110. https://doi.org/10.1016/j.pecs.2012.05.003.

[12] Shioyoke, A., Hayashi, J., Murai, R., Nakatsuka, N., and Akamatsu, F., "Numerical Investigation on Effects of Nonequilibrium Plasma on Laminar Burning Velocity of Ammonia Flame," *Energy and Fuels*, Vol. 32, No. 3, 2018, pp. 3824–3832. https://doi.org/10.1021/acs.energyfuels.7b02733.

[13] Taneja, T. S., and Yang, S., "Numerical modeling of plasma assisted pyrolysis and combustion of ammonia," *AIAA Scitech 2021 Forum*, , No. January, 2021, pp. 1–9. https://doi.org/10.2514/6.2021-1972.

[14] Faingold, G., and Lefkowitz, J. K., "A numerical investigation of NH3/O2/He ignition limits in a non-thermal plasma," *Proceedings of the Combustion Institute*, Vol. 38, No. 4, 2021, pp. 5849–5857. https://doi.org/10.1016/j.proci.2020.08.033.

[15] Choe, J., Sun, W., Ombrello, T., and Carter, C., "Plasma assisted ammonia combustion: Simultaneous NOx reduction and flame enhancement," *Combustion and Flame*, Vol. 228, 2021, pp. 430–432. https://doi.org/10.1016/j.combustflame.2021.02.016.

[16] Shahsavari, M., Konnov, A. A., Valera-Medina, A., and Jangi, M., "On nanosecond plasma-assisted ammonia combustion: Effects of pulse and mixture properties," *Combustion and Flame*, Vol. 245, 2022, p. 112368. https://doi.org/10.1016/j.combustflame.2022.112368.

[17] Qiu, Y., Zhu, Y., Wu, Y., Zhao, N., Li, Z., Hao, M., Zhang, B., and Pan, D., "Numerical investigation of the hybrid pulse–DC plasma assisted ignition and NOx emission of NH3/N2/O2 mixture," *Combustion and Flame*, Vol. 258, 2023. https://doi.org/10.1016/J.COMBUSTFLAME.2023.113078.

[18] Sun, J., Bao, Y., Ravelid, J., Nilsson, S., Konnov, A. A., and Ehn, A., "Application of emission spectroscopy in plasma-assisted NH3/air combustion using nanosecond pulsed discharge," *Combustion and Flame*, Vol. 263, 2024, pp. 10–2180. https://doi.org/10.1016/j.combustflame.2024.113400.

[19] Mao, X., Zhong, H., Liu, N., Wang, Z., and Ju, Y., "Ignition enhancement and NOx formation of NH3/air mixtures by non-equilibrium plasma discharge," *Combustion and Flame*, Vol. 259, 2024, p. 113140. https://doi.org/10.1016/J.COMBUSTFLAME.2023.113140.

[20] Shanbhogue, S. J., Dijoud, R. J., Pavan, C. A., Rao, S., Campo, F. G. D., Guerra-Garcia, C., and Ghoniem, A. F., "Emissions and Dynamic Stability Improvements in Premixed CH4/NH3 Swirling Flames with Nanosecond Pulsed Plasmas," *AIAA Aviation Forum and ASCEND 2024*, 2024. https://doi.org/10.2514/6.2024-3898.

[21] Pavan, C. A., and Guerra-Garcia, C., "Modelling the Impact of a Repetitively Pulsed Nanosecond DBD Plasma on a Mesoscale Flame," *AIAA Science and Technology Forum and Exposition, AIAA SciTech Forum 2022*, 2022, pp. 1–13. https://doi.org/10.2514/6.2022-0975.

[22] Pavan, C., "Nanosecond Pulsed Plasmas in Dynamic Combustion Environments," Ph.D. thesis, Massachusetts Institute of Technology, Cambridge, USA, 2023. URL https://dspace.mit.edu/handle/1721.1/151492.

[23] Dijoud, R. J., *Ignition by Nanosecond Repetitively Pulsed Discharges*, S.M. thesis, Massachusetts Institute of Technology, Cambridge, USA, 2023. URL https://dspace.mit.edu/handle/1721.1/154175.

[24] Dijoud, R. J., and Guerra-Garcia, C., "Numerical model of the initiation and propagation of a radial flame front by NRP discharge," *AIAA Science and Technology Forum and Exposition 2023*, 2023. https://doi.org/10.2514/6.2023-0747.

[25] Dijoud, R. J., Pavan, C. A., and Guerra-Garcia, C., "Parametric Exploration of Radial Ignition by Nanosecond Repetitively Pulsed Discharges," *AIAA Science and Technology Forum and Exposition 2024*, 2024. https://doi.org/10.2514/6.2024-0181.

[26] Dijoud, R. J., Laws, N., and Guerra-Garcia, C., "Mapping the performance envelope and energy pathways of plasma-assisted ignition across combustion environments," *Combustion and Flame*, Vol. 271, 2025, p. 113793. https://doi.org/10.1016/J.COMBUSTFLAME.2024.113793.

[27] Hagelaar, G. J., and Pitchford, L. C., "Solving the Boltzmann equation to obtain electron transport coefficients and rate coefficients for fluid models," *Plasma Sources Science and Technology*, Vol. 14, No. 4, 2005, pp. 722–733. https://doi.org/10.1088/0963-0252/14/4/011.

[28] Pancheshnyi, S., Eismann, B., Hagelaar, G. J., and Pitchford, L. C., "Computer code ZDPlasKin," , 2008. URL http://www.zdplaskin.laplace.univ-tlse.fr.

[29] Goodwin, D. G., Moffat, H. K., Schoegl, I., Speth, R. L., and Weber, B. W., "Cantera: An object-oriented software toolkit for chemical kinetics, thermodynamics, and transport processes (version 2.6.0)," , 2022. https://doi.org/10.5281/zenodo.6387882, URL https://www.cantera.org.

[30] Mcbride, B. J., Zehe, M. J., and Gordon, S., "NASA Glenn Coefficients for Calculating Thermodynamic Properties of Individual Species," Tech. rep., TP-2002-211556, NASA Glenn Research Center, Cleveland, OH, USA, 2002.

[31] Zhong, H., Mao, X., Liu, N., Wang, Z., Ombrello, T., and Ju, Y., "Understanding non-equilibrium N2O/NOx chemistry in plasma-assisted low-temperature NH3 oxidation," *Combustion and Flame*, Vol. 256, 2023, p. 112948. https://doi.org/10.1016/J.COMBUSTFLAME.2023.112948.